

UC San Diego

UC San Diego Electronic Theses and Dissertations

Title

Conversion Reactions of Transition Metal Chlorides

Permalink

<https://escholarship.org/uc/item/0xc7n7ww>

Author

Kim, Seonghyun

Publication Date

2017

Peer reviewed|Thesis/dissertation

UNIVERSITY OF CALIFORNIA, SAN DIEGO

Conversion Reactions of Transition Metal Chlorides

A thesis submitted in partial satisfaction of the requirements
for the degree Master of Science

in

Chemical Engineering

by

Seonghyun Kim

Committee in charge:

Professor Ping Liu, Chair
Professor Zheng Chen
Professor Jian Luo

2017

Copyright

Seonghyun Kim, 2017

All rights reserved.

The Thesis of Seonghyun Kim is approved, and it is acceptable in quality and form for publication on microfilm and electronically:

Chair

University of California, San Diego

2017

DEDICATION

To my parents,

Dong Sig Kim and Gi Yeon Kim

TABLE OF CONTENTES

Signature Page	iii
Dedication	iv
Table of Contents	v
List of Figures	vii
List of Tables	ix
Acknowledgements	x
Abstract of Thesis	xi
Chapter 1. Li-ion Batteries.....	1
1.1. Energy Density.....	1
1.2. Battery Reactions	4
1.3. Configurations.....	6
1.4. Limitations	8
Chapter 2. Conversion Reactions of Transition Metal Chlorides	11
2.1. Introduction.....	11
2.1.1. Conversion Cathode Materials.....	11
2.1.2. Superconcentrated Electrolytes.....	15
2.1.3. LiNO ₃ Additives	17
2.2. Results & Discussion	18

2.2.1. Effect of Solvents (1 st screening).....	18
2.2.2. Effect of Electrode Materials (2 nd screening)	22
2.2.3. Electrochemical Analysis.....	28
2.2.4. Characterizations.....	38
2.3. Methods.....	46
2.4. Conclusion	47
References.....	49

LIST OF FIGURES

Figure 1.1	Ragone Plot of Batteires ^[2]	2
Figure 1.2	Characteristics of HEV, PHEV, EV in terms of battery properties ^[3]	3
Figure 1.3	Li-ion battery configuration in charge/discharge Li ion mobility	5
Figure 1.4	Representative anode material forms and their dis/advantages ^[12]	10
Figure 2.1	Transition metal chloride dissolution test in each solvent: (a) FeCl ₃ , (b) FeCl ₂ , (c) CoCl ₂ , (d) NiCl ₂ , (e) MnCl ₂ in pure LP30 (EC:DME = 1:1 with 1M LiPF ₆), pure DME, pure TEGDME, 0.1M LiCl LP30, 0.1M LiCl DME, 0.1M LiCl TEGDME, and 0.1M LiCl/6M LiTFSI TEGDME	20
Figure 2.2	Open Circuit Voltage (OCV) of metal chloride materials in (a) reference electrolyte, (b) 0.1M LiCl/6M LiTFSI TEGDME, and (c) 0.1M LiCl/0.1M LiNO ₃ /6M LiTFSI TEGDME	24
Figure 2.3	Voltage profile of FeCl ₃ in (a) 0.1M LiCl/6M LiTFSI TEGDME, and (b) 0.1M LiCl/0.1M LiNO ₃ /6M LiTFSI TEGDME	25
Figure 2.4	Voltage profile of FeCl ₂ in (a) 0.1M LiCl/6M LiTFSI TEGDME, and (b) 0.1M LiCl/0.1M LiNO ₃ /6M LiTFSI TEGDME	26
Figure 2.5	Voltage profile of MnCl ₂ in (a) 0.1M LiCl/6M LiTFSI TEGDME, and (b) 0.1M LiCl/0.1M LiNO ₃ /6M LiTFSI TEGDME	27
Figure 2.6	Voltage profile of CoCl ₂ in (a) reference electrolyte, (b) 0.1M LiCl/6M LiTFSI TEGDME, and (c) 0.1M LiCl/0.1M LiNO ₃ /6M LiTFSI TEGDME	30
Figure 2.7	Cycling performance of CoCl ₂ in (a) 0.1M LiCl/6M LiTFSI TEGDME, and (b) 0.1M LiCl/0.1M LiNO ₃ /6M LiTFSI TEGDME	31
Figure 2.8	Voltage profile of NiCl ₂ in (a) reference electrolyte, (b) 0.1M LiCl/6M LiTFSI TEGDME, and (c) 0.1M LiCl/0.1M LiNO ₃ /6M LiTFSI TEGDME	34

Figure 2.9	Cycling performance of NiCl ₂ in (a) 0.1M LiCl/6M LiTFSI TEGDME, and (b) 0.1M LiCl/0.1M LiNO ₃ /6M LiTFSI TEGDME	35
Figure 2.10	Galvanostatic Intermittent Titration Technique (GITT) of (a) CoCl ₂ , and (b) NiCl ₂ in 0.1M LiCl/0.1M LiNO ₃ /6M LiTFSI TEGDME	37
Figure 2.11	X-Ray Diffraction (XRD) characterizations of (a) CoCl ₂ , and (b) NiCl ₂	42
Figure 2.12	Vibrating Sample Magnetometer (VSM) characterizations of CoCl ₂ of (a) as prepared electrode, (b) after discharged, (c) after recharged	43
Figure 2.13	Vibrating Sample Magnetometer (VSM) characterizations of NiCl ₂ of (a) as prepared electrode, (b) after discharged, (c) after recharged	44
Figure 2.14	Fourier-Transform Infrared Spectroscopy (FT-IR) of CoCl ₂	45

LIST OF TABLES

Table 1.	Representative intercalation and conversion material properties	13
Table 2.	Dissolution results of metal chloride materials in different electrolytes (+): insoluble, (-): soluble	21

ACKNOWLEDGEMENTS

Firstly, I would like to thank to my thesis advisor Professor Ping Liu for providing me all the opportunities to do this research and his support. Through countless discussion, advice, and encouragement, his appropriate guidance has proved to be invaluable. I would also like to express my appreciation to my other committee members: Dr. Jian Luo, and Dr. Zheng Chen for their time and guidance.

Secondly, I would like to acknowledge Dr. Hee-Dae Lim whom I had many discussions. I also expand my gratitude to all my group members in Liu research group who have helped, commented, and inspired me in successfully proceeding my research.

Last but not least, my deepest gratitude goes to my parents Dong Sig Kim and Gi Yeon Kim for their abundant belief and support. I would also like to express my special appreciation to Michelle for her endless support and encouragement through graduate school.

ABSTRACT OF THE THESIS

Conversion Reactions of Transition Metal Chlorides

by

Seonghyun Kim

Master of Science in Chemical Engineering

University of California, San Diego, 2017

Professor Ping Liu, Chair

Li-ion batteries have become an attractive key component in energy storage systems as the worldwide energy infrastructure shifts towards being more environmentally concerned. The development of Li-ion batteries has also been pressured from the rapid growth of modern technologies such as mobile electronic device and an electric vehicle based transportation society. However, unlike the fast pace development of other aspects of these technologies, the development of better Li-ion batteries has

remained a limiting factor. Therefore, today's technology market demands the appearance of new Li-ion battery system with higher energy density. To satisfy this demand, Li-ion batteries must advance beyond intercalation cathode materials. Transition metal chloride cathode conversion materials show promise of a new paradigm in energy storage system due to their relatively high energy density. However, disintegration of metal chlorides remains a critical issue in application to a battery.

In this thesis, highly concentrated electrolytes that consist of 0.1M LiCl/6M LiTFSI and 0.1M LiCl/0.1M LiNO₃/6M LiTFSI in TEGDME solvent is introduced to effectively suppress the dissolution of cathode materials. Among metal chloride materials, CoCl₂ and NiCl₂ show promise with high capacities of 160 mAh g⁻¹ and 330 mAh g⁻¹, up to 40% and 80% of their theoretical capacities respectively, in a superconcentrated electrolyte with LiNO₃ additive introduced to protect the lithium surface. NiCl₂ in a properly treated electrolyte (0.1M LiCl/0.1M LiNO₃/6M LiTFSI in TEGDME) showed the most promising behavior with stable cycling and low hysteresis ~ 0.5 V as a new positive electrode material to replace intercalation based rechargeable battery.

Chapter 1. Li-ion Batteries

1.1. Energy Density

Rechargeable Li-ion batteries are non-substitutable energy storage systems required by today's informational mobile and transportation society due to their portable, environment-friendly, and high energy density properties. Li-ion batteries have outstanding performance in energy density and power density compare to previous Lead-acid, Nickel-Cadmium(Ni-Cd), and Nickel-Metal Hydride(Ni-MH) batteries. Lead-acid batteries were the first rechargeable batteries to be commercialized by Planté in 1859 with a specific energy density less than 30 Wh kg^{-1} , and volumetric energy density less than 100 Wh l^{-1} [1]. Modern Li-ion batteries provide a drastic improvement to battery energy density, providing more than 200 Wh kg^{-1} of specific energy density and 350 Wh l^{-1} of volumetric energy density (Fig. 1.1). While Ni-MH batteries are promising batteries for hybrid electric vehicle (HEV) with their high stability, high energy density and power density Li-ion batteries are more suitable as the plug-in hybrid electric vehicle (PHEV) and electric vehicle (EV) market expands (Fig. 1.2). Since the rate of progress in computer industry boosts the demand for the battery improvement such as fast-charge, lightweight, and high capacity and energy density, Li-ion batteries are considered as essential energy storage systems. Moreover, the environmental regulations in automobile market and industry are getting stricter every year, making development of new battery systems becomes more crucial.

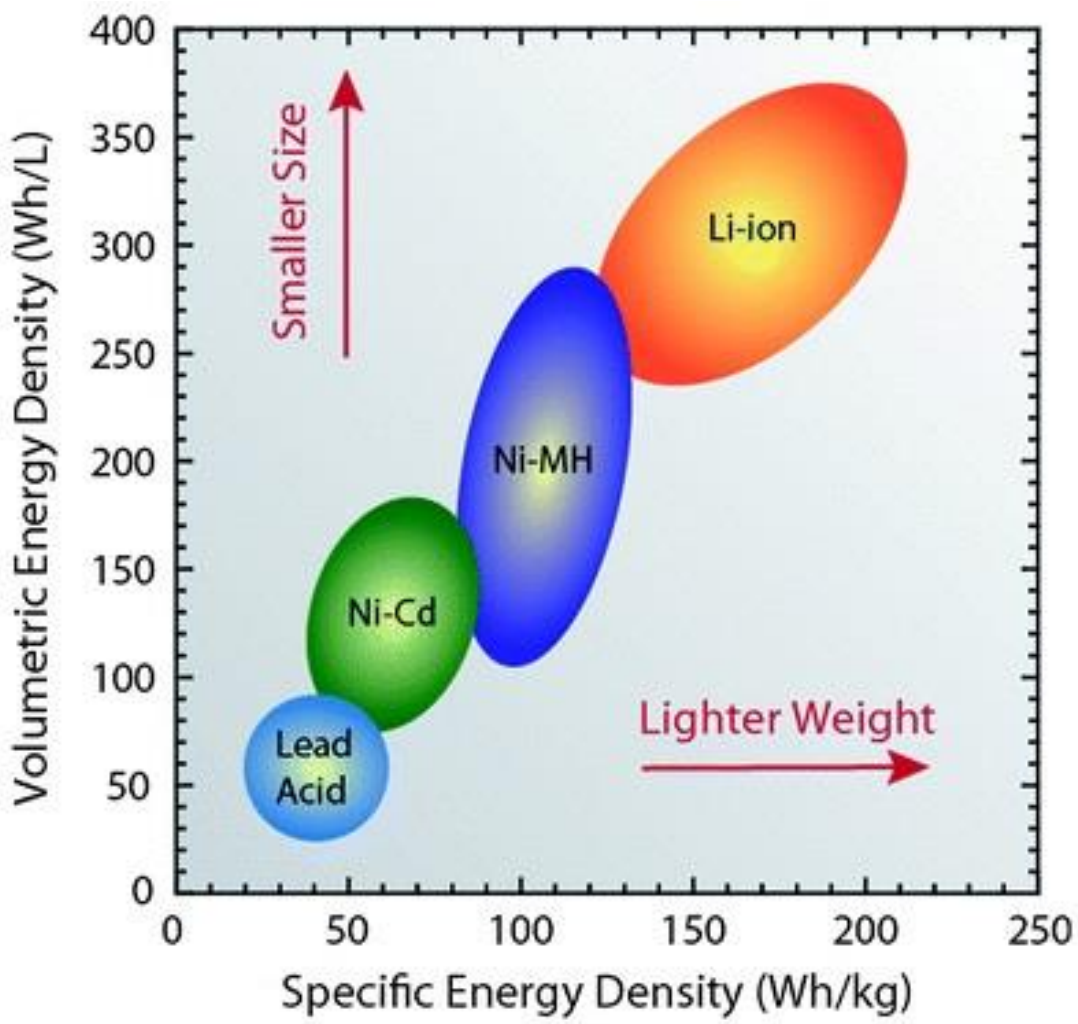


Figure 1.1 Ragone Plot of Batteries^[2]




Modes of operation	battery capacity needed, kWh	Energy density, Wh/kg	Weight of battery, Kg	Speed, kilometres per hour	Distance on one charge, kilometres
 Hybrid	<3	40-50 (Ni-MH)	60 (Ni-MH)	100+	15
 Plug in Hybrid	5.6-18	90-100 (Li-ion)	60-200 (Li-ion)	100+	10-60
 Full EV	35-54	90-100 (Li-ion)	450 (Li-ion)	>100	150-200

Figure 1.2 Characteristics of HEV, PHEV, EV in terms of battery properties^[3]

1.2. Battery Reactions

Rechargeable batteries structurally consist of cathode and anode electrodes with a separator and electrolyte, and are required to successfully charge and discharge while maintaining a stable electrochemistry during repeated lithiation/delithiation, in the case of lithium ion batteries with intercalation electrode materials. An electrolyte facilitates the ion transport throughout the cells and must be thermodynamically stable at the battery operating potentials (Fig. 1.3). Electrode materials and ions determine the maximum amount of energy storage where lithium ion batteries have a working potential over 3 V and high energy density^[1]. Batteries convert chemical energy to electric energy, and vice versa by a redox mechanism. Oxidation occurs at anode during discharge ($A \rightarrow A^+ + e^-$), and reduction occurs at cathode ($C^+ + e^- \rightarrow C$). During discharge, reduction occurs when electrons from anode migrate to electric devices through the electric circuit, and arrive at cathode materials. At the same time, lithium ion migrates from anode materials to cathode through the electrolyte.

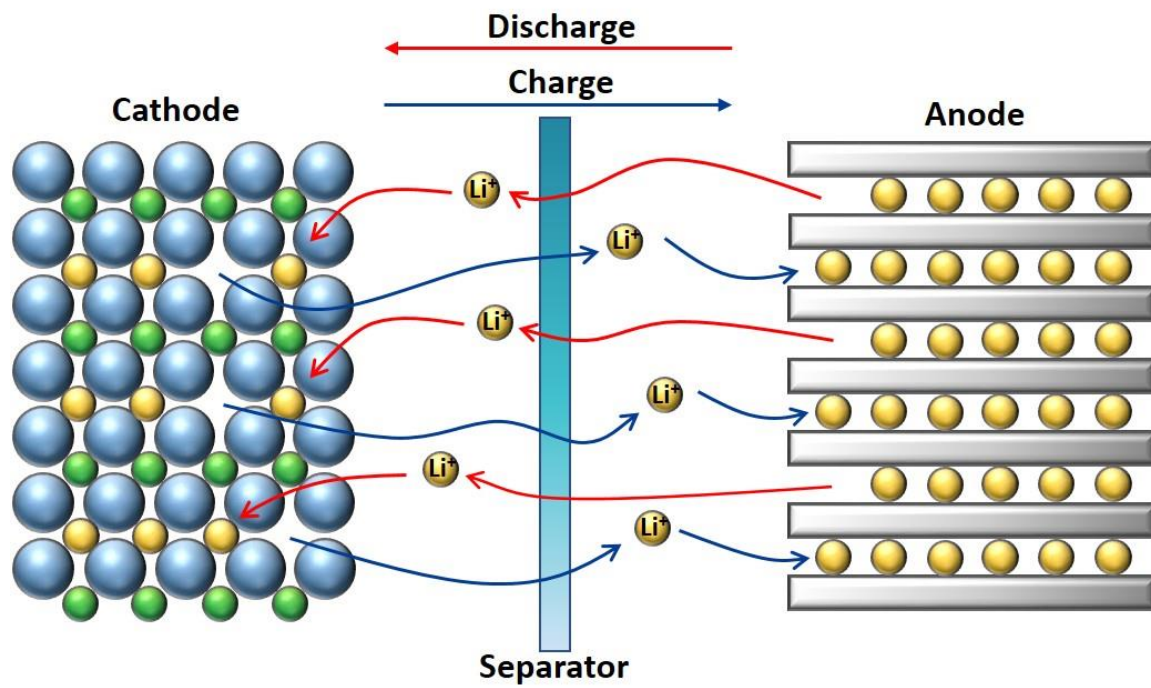


Figure 1.3 Li-ion battery configuration in charge/discharge Li ion mobility

1.3. Configurations

Cathode

Commercialized cathode materials generally function through an intercalation mechanism, for example LiCoO_2 ^[4], by inserting and ejecting lithium ions into/from the CoO_2^- layer gaps^[5]. Cathode materials require stable and reversible high potential intercalation-deintercalation reactions, while minimizing nonreversible side reactions. They also require high electric and ionic conductivity to maintain a low internal resistance for high efficiency and power output. Chemical/electrochemical and thermal stability are also required to maintain great cycling performance.

Anode

Anode materials require low potential, structural stability during cycling, reversibility with high coulombic efficiency, high diffusion rate and electric/ionic conductivity, and high capacity and energy density to store lithium ions. Lithium metal was used as anode due to its high capacity and low potential that enables a large cell voltage range, but lithium metal is extremely reactive to water and forms dendrite during cycling that shorten the cell lifetime. To overcome the problems of Lithium metal, graphite is commonly used as the anode because of its stable intercalation structure that enables lithiation/delithiation with low deformations and a low potential close to lithium metal. Graphite anode enables the long lifecycle of Li-ion batteries with reversible redox reactions at a potential of 0.00 ~ 0.25 V (vs. Li^+/Li) with a theoretical capacity of 372 mAh g^{-1} ^[1].

At the interface between electrolyte and anode surface, electrolyte decomposes during charge since the potential of electrolyte is higher than that of anode material. This results in the formation of solid electrolyte interphase (SEI) layer. SEI layer passivates the anode surface and prevents further decomposition of electrolytes. Moreover, SEI helps battery safety. However, SEI leads high internal resistance, self-discharge, capacity loss, and low efficiency causing degradation of battery performance. Therefore, there are a lot of research going on SEI formation to optimize the battery configuration^[6].

Although graphite anode is widely used for commercial batteries, anode materials require higher capacity to drastically improve the battery performance. Thus, some non-carbon anode materials with high capacity, for example Silicon (Si) and Tin (Sn), are proposed to replace graphite anode^[7, 8]. Other than graphite intercalation, alloy or conversion form of anode materials are considered as another category of anode materials with high capacity and relatively low average voltage.

Electrolytes

Electrolytes, as ion transport medium, consist of solvents and salts. Ionic conductivity is one of the most important factors that electrolytes must have since electrolytes help ions to move between anode and cathode. To induce the best performance of electrode active materials, proper selection of electrolytes optimized to the electrodes is necessary. Electrolytes are categorized in three different phases: liquid electrolytes, solid electrolytes, polymer electrolytes^[1]. In commercial Li-ion batteries, liquid organic electrolytes are often used. Electrolytes require high ionic conductivity, chemical/electrochemical stability, wide temperature range, and need to be safe to use. In

order to have a high ionic conductivity, electrolytes need to have high dielectric constant to dissolve more lithium salts to help ionic mobilization. Lithium hexafluorophosphate (LiPF_6) is a common salt in Li-ion batteries since it has high solubility in solvents, high chemical stability, and high ionic conductivity^[9]. However, LiPF_6 has a poor thermal stability, and it possesses a safety issue by forming Hydrofluoric acid (HF) with a little amount of moisture^[10].

1.4 Limitations

Commercialized Li-ion batteries are widely used in variety of applications nowadays, yet Li-ion batteries are the limiting factors in terms of the pace of technology development. Among electrodes, electrolytes, separators, and current collectors, optimizations and highly compatible combinations are required to improve the cell performance. Positive and negative electrode materials, and the interface between electrodes and electrolyte are the determining factors for the battery performance no matter the type of battery. However, unlike lead-acid or Ni-Cd batteries, Li-ion batteries still have room to mature over the next decades. The key improvement for the next Li-ion batteries will be on the intrinsic change of electrochemistry and engineering design.^[11]

Other than graphite intercalation anodes, alloy and conversion chemistry anodes have shown great potential to increase the cell capacity and energy density, but still have significant challenges to overcome before commercialization (Fig. 1.4). Alloy anodes have been investigated and successfully commercialized in some fields, but still requires more studies at an applicable level. However, unlike anode materials, other forms besides intercalation based cathode materials have not yet been developed. To step forward into

the next generation of Li-ion batteries, drastic increase of cell capacity is necessary with a change of electrochemistry, for example, by replacing intercalation to cathode conversion reaction materials.

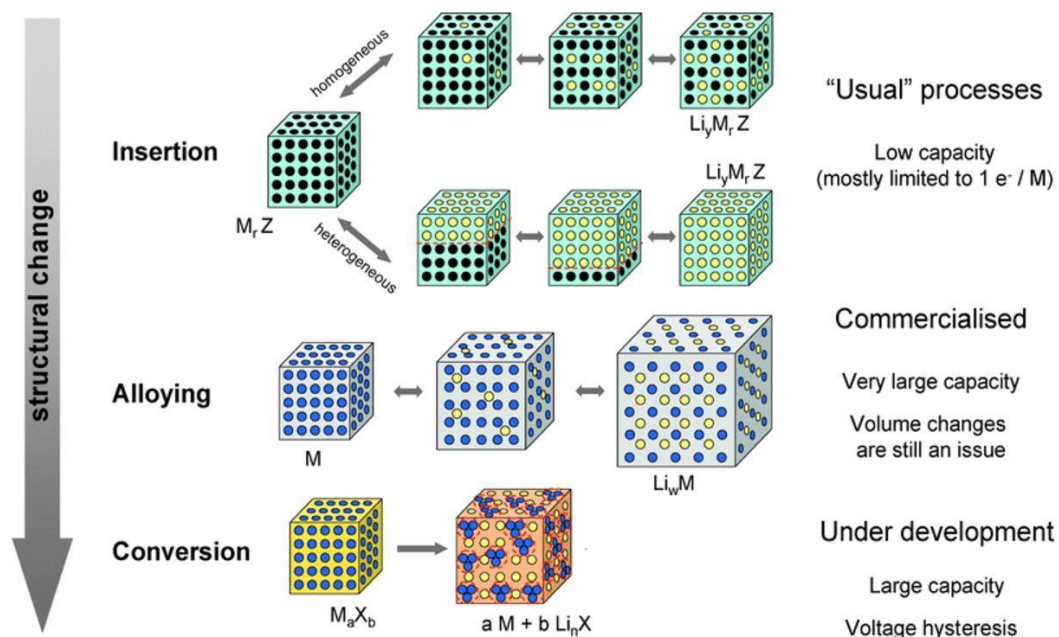


Figure 1.4 Representative anode material forms and their dis/advantages^[12]

Chapter 2. Conversion Reactions of Transition Metal Chlorides

2.1. Introduction

2.1.1. Conversion Cathode Materials

The general conversion material form is an oxide anode active material with extremely high gravimetric and volumetric capacity at low potential. Since most oxide forms of conversion materials have potentials below 1 V, conversion materials are often attractive candidates for anode. Furthermore, some conversion materials such as transition metal chlorides or fluorides are considered as intercalation-replaceable cathode materials with their high capacity. During lithiation/delithiation in halogens and metal halides, a solid-state redox reaction takes place by breaking and reforming the chemical bonds through the following equation:



Where M^{y+} = cation, M = reduced cation metal, X = anion.

Unlike intercalation lithiation/delithiation (limited electron transfer to $0.5 e^-$), more than one electron transfers in each metal, resulting in large capacity^[13]. Transition metal chloride or fluoride conversion materials have moderate to high potentials, and thus they are classified as promising cathode materials. Metal fluoride materials have relatively higher theoretical gravimetric and volumetric capacities than metal chlorides, and thus, metal fluorides have been heavily studied for high energy density applications. However, during lithiation/delithiation, fluorine can formulate HF by reacting with a proton stripped from the organic electrolyte and moisture^[10]. Highly toxic HF can cause serious safety

issues in using batteries. HF not only shortens the battery lifetime, but is also harmful to battery users if a leak occurs. More importantly, high hysteresis is one of the major issues in using metal fluoride conversion materials. In metal fluoride conversion reactions, for example, FeF_3 produces LiF salt in reversible reaction as a following equation: $\text{FeF}_{3(s)} + \text{Li} \leftrightarrow \text{Fe}_{(s)} + \text{LiF}_{(s)}$. The three solid materials present in the conversion reaction cause high hysteresis of about 1 V^[14]. A basic hypothesis that drives this Thesis is that if the lithium salt can be partially dissolved into the electrolyte, the hysteresis can be reduced which is essential for practical applications of conversion cathodes in batteries. Since it is hard to find a salt that can partially dissolve LiF(s) and lower the hysteresis, metal chloride materials are favored since it is expected LiCl can partially dissolve resulting in lower the hysteresis. Therefore, relatively safer and lower hysteresis metal chlorides with high capacities are investigated throughout this paper.

Transition metal chlorides are promising conversion cathode materials with high theoretical capacities, and energy densities compared to commercial intercalation cathode materials as seen in the Table 1. Their potentials are also high enough for use in devices that operate in a moderate voltage range.

Table 1. Representative intercalation and conversion material properties

Type	Materials	Theoretical Potential (V)	Theoretical Gravimetric Capacity (mAh g ⁻¹)	Theoretical Volumetric Capacity (mAh cm ⁻³)	Theoretical Energy Density (Wh kg ⁻¹)	Theoretical Energy Density (Wh L ⁻¹)
Intercalation	LiFePO ₄	3.4	170	612	580	2088
	LiCoO ₂	3.8	272	1387	1033	5268
Conversion	FeCl ₃	2.83	495.7	1437.5	1403	4068.7
	FeCl ₂	2.41	423	1336.7	1020	3223.2
	CoCl ₂	2.59	412.8	1387	1092	3669
	NiCl ₂	2.64	413.6	1468.3	1065	3781
	MnCl ₂	3.38	426	1270	1440	4291

However, transition metal chlorides have serious problems that need to be resolved before commercialization, despite of their attractive properties. The major challenges include low conductivity, large voltage hysteresis, volume changes during cycling, and side interactions between active materials and electrolytes^[15]. Low conductivity causes capacity loss. Poor kinetics and reversibility, large voltage hysteresis causes low efficiency. Volume changes and side interaction cause poor cycling and coulombic efficiency^[15, 16]. More significantly, dissolution of active materials is one of the major issues and results in shuttling of dissolved species, re-precipitation of cathode compounds, and increase of cell resistance due to the blockage of ionic pathway by contacting anode surface, all which cause serious capacity and rate performance drops. To resolve the dissolution issue, modification and optimization of electrolyte is necessary. Since it is reported that ether-based solvents are less polar than carbonate electrolytes^[17], ether-based electrolyte is more suitable for metal chloride cathodes. Highly concentrated electrolyte can be the best approach to minimize the cathode material dissolution. When there are no “free” solvent molecules left in the electrolyte^[18-20] and when lithium salt solvation energy is much higher than that of dissolved cathode materials^[19, 20], it ideally prevents unwanted reactions between electrolyte and cathode species. As an additional approach, electrolyte additives can improve the cell performance by forming favorable SEI layer to protect the lithium surface. In this research, lithium nitrate (LiNO_3) was chosen to induce the passivation layer formation on anode electrodes to show the improvement of ionic conductivity and preventability of surface reactions with electrolyte.

2.1.2. Superconcentrated Electrolytes

The major challenge of transition metal chlorides applications to batteries is that transition metal chloride materials have very high solubility in normal carbonate electrolytes. Even though their theoretical properties have great promises, dissolution is a critical problem causing a loss of cathode active materials, undesired side reactions, and a reduction at the lithium metal which results in drastic drop of coulombic efficiency and cell capacity^[21]. For the appropriate application of metal chloride cathode materials, development of a new design of electrolyte is necessary. Since metal chloride is ionized when it dissolves in electrolytes, addition of lithium chloride (LiCl) is proposed to suppress decomposition of metal chloride ionizations. In addition, superconcentrated electrolytes effectively suppress transition metal dissolution, thus enabling safer and more stable electrolyte design at high voltages^[22].

In commercial Li-ion batteries, LiPF₆ is the most commonly used salt due to its great balance of properties, proper formation of SEI on graphite or silicon anode, and passivation layer on the aluminum current collector of cathodes^[9, 23, 24], regardless of relatively low ionic conductivity, sensitivity to hydrolysis, and poor thermal stability required for batteries^[25]. However, using LiPF₆ as a salt in an electrolyte for a battery with cathode transition metal chlorides is not suitable since fluorine species (i.e. LiPF₆ or LiBF₄) cause dissolution of cathode material in carbonate electrolytes^[26]. Instead, lithium bis(trifluoromethanesulfonyl)imide (LiTFSI) is an appealing candidate to use as a salt with its highly soluble properties. For an effective highly concentrated electrolyte, Tetraethylene glycol dimethyl ether (TEGDME or tetraglyme or G4) has a great advantage as a new electrolyte with LiTFSI. Highly concentrated electrolytes have lower ionic conductivity

and higher viscosity compared to conventional 1M electrolytes which impede battery rate performance^[27]. However, they have sufficient advantages to make them attractive as electrolytes: great reductive stability to facilitate reversible reactions of low potential negative electrodes, great oxidative stability to suppress corrosion on Al current collector without help of fluorine species, low volatility and high thermal stability to improve battery safety, high carrier density, fast electrode reaction, and suppression of polysulfide dissolution on positive electrode to enhance sulfur battery performance^[27].

2.1.3. LiNO₃ Additives

Superconcentrated electrolyte seems very attractive, but it will not solve the ultimate dissolution problem alone. In lithium sulfur battery research, the dissolution of polysulfide is also the most critical problem to solve, and LiNO₃ is a common additive to prevent the loss of coulombic efficiency and capacity^[28, 29]. There are many reports that try to prove the effect of LiNO₃ additive either of suppressing polysulfides at cathode region^[30], or of the formation of passivation layer on Lithium surface at anode region^[31-33]. However, researches are mostly focused on the effect of LiNO₃ at anode Lithium surface. Mikhylik^[31] first applied the concept to a Li-S battery, and Aurbach^[32] and Liang^[33] proved the effect of LiNO₃. When LiNO₃ is added to the electrolyte, it has a high favorability to react on the lithium metal to form an in situ protective layer, acting as a SEI between lithium metal and the Li-ion battery electrolyte (polar-aprotic solutions)^[31, 32]. This surface passivation film has a high Li ion transfer, but it blocks electrons under an electric field, resulting in preventing electrode corrosion from the dissolved polysulfides, or from the chlorides in the case of transition metal chloride^[28, 31, 33]. More importantly, the surface protective layer works as an obstacle to stop the direct contact between lithium metal and the dissolved cathode species in the electrolyte^[33]. However, LiNO₃ may cause electrochemical instability due to its irreversible reduction on cathode region at low potentials, side reactions, and safety issues due to its strong oxidative property^[29, 34]. However, in using transition metal chloride cathode materials, degradation is the most critical issue (similarly to lithium sulfur batteries) making it worthwhile to use LiNO₃ additives to improve coulombic efficiency and battery capacity by protecting the lithium anode surface from the direct contact of dissolved cathode materials.

2.2. Results & Discussion

2.2.1. Effect of Solvents (1st screening)

Prior to the selection of electrolyte solvents, dissolution test of transition metal chlorides in each solvent was first conducted by detecting the color change of electrolytes (Fig. 2.1 and Table 2). The base electrolyte solvents were prepared as following: LP30 (EC:DME = 1:1 with 1M LiPF₆), Dimethoxyethane (DME), TEGDME. In each solvent, 0.1M of LiCl was dissolved in order to see the effect of chloride dissolution suppression. Finally, in TEGDME with 0.1M LiCl, 6M of LiTFSI was added to make SIL. The amount of FeCl₃ varied, but it was well dissolved in all the solvents including SIL, showing light to dark yellow colors (Fig. 2.1 (a)). FeCl₂ did not have a color when it dissolved in the solvents, but the dissolved FeCl₂ affected the cloudiness of the solvents (Fig. 2.1 (b)). Solvents became more cloudy in pure LP30, pure DME, and 0.1M LiCl DME than in Pure TEGDME, 0.1M LiCl LP30, 0.1M TEGDME, and SIL, which led us to conclude that FeCl₂ had the lowest solubility in TEGDME based solvents. Sky blue colored CoCl₂ powder was tested in each solvent, and CoCl₂ was well dissolved in most of solvents except pure DME and SIL TEGDME. In pure DME, CoCl₂ had a low solubility, but it still showed some color change, while CoCl₂ powder kept its sky blue color in SIL TEGDME. NiCl₂ was highly soluble in most of solvents except SIL TEGDME as well. MnCl₂ dissolved in DME type solvents with cloudy color, but it had a low solubility in LP30 and TEGDME solvents. The dissolution results are summarized in Table 2. Overall, 0.1M LiCl/6M LiTFSI SIL TEGDME showed the best performance in suppressing dissolution of metal chloride electrode materials, and this solvent was selected as the most promising electrolyte for

further experiments. To verify the effect of LiNO_3 additive in the electrolyte, 0.1M LiNO_3 was added in 0.1M $\text{LiCl}/6\text{M LiTFSI}$ TEGDME as a second electrolyte. Also, the reference electrolyte was made with TEGDME based solvent including 1M LiTFSI .



Figure 2.1 Transition metal chloride dissolution test in each solvent: (a) FeCl_3 , (b) FeCl_2 , (c) CoCl_2 , (d) NiCl_2 , (e) MnCl_2 in pure LP30 (EC:DME = 1:1 with 1M LiPF_6), pure DME, pure TEGDME, 0.1M LiCl LP30, 0.1M LiCl DME, 0.1M LiCl TEGDME, and 0.1M LiCl/6M LiTFSI TEGDME.

Table 2. Dissolution results of metal chloride materials in different electrolytes.

(+): insoluble, (-): soluble

Materials	Pure			0.1M LiCl			0.1M LiCl/6M LiTFSI
	LP30	DME	TEGDME	LP30	DME	TEGDME	TEGDME
FeCl ₃	-	-	-	-	-	-	-
FeCl ₂	-	-	+	+	-	+	+
CoCl ₂	-	-	-	-	-	-	+
NiCl ₂	-	-	-	-	-	-	+
MnCl ₂	+	-	+	+	-	+	+

2.2.2. Effect of Electrode Materials (2nd screening)

After the first screening, reference electrolyte (1M LiTFSI TEGDME), and two other electrolytes (0.1M LiCl/6M LiTFSI TEGDME, and 0.1M LiCl/0.1M LiNO₃/6M LiTFSI TEGDME) were selected to test the electrode candidates. Another screening of the five candidates, FeCl₃, FeCl₂, CoCl₂, NiCl₂, and MnCl₂, was necessary to decide which electrode materials were actually comparable to those selected electrolytes. To screen out the unpromising electrode materials, Open Circuit Voltage (OCV) was first tested to see the stability in each electrolyte. The following experiment was carried out to evaluate how the SIL suppress the dissolution of metal chloride cathode materials: OCV was monitored for 30 h to detect the self-discharge and the voltage drops of each cell (Fig. 2.2).

In Fig. 2.2 (a), all the electrode materials had voltage drops. FeCl₃, FeCl₂, CoCl₂ continuously dropped ~ 1 V, ~ 1.2 V, ~ 0.6 V, respectively, and NiCl₂ and MnCl₂ dropped ~ 0.2 V, and ~ 0.3 V, respectively. Significant voltage drops indicates that the electrolyte allows the dissolution of metal chlorides which results in internal shorts^[35]. CoCl₂, NiCl₂, MnCl₂ have highly stable OCV in superconcentrated SIL electrolyte, on the other hand, both FeCl₃ and FeCl₂ showed more significant voltage drops, ~ 2.0 V, than reference electrolytes (Fig. 2.2 (b)). Similarly, CoCl₂, NiCl₂, and MnCl₂ showed stable OCV in the superconcentrated electrolyte containing LiNO₃ additive.

To confirm the electrochemical performance of each electrode before eliminating from the list, the voltage profile and cycling performance were obtained (Fig. 2.3, 2.4, 2.5). In the superconcentrated electrolyte without additive, FeCl₃ showed 4 cycles with low capacity around 15 mAh g⁻¹ at the first discharge (Fig. 2.3 (a)), but cell did not perform in the electrolyte containing additive. FeCl₂ showed more than 5 cycles, but it showed a low

capacity, that is 13% of theoretical capacity at most (Fig. 2.4). MnCl_2 was screened out even though it had a stable OCV due to its poor electrochemical performance in superconcentrated electrolytes (Fig. 2.5). Therefore, from the electrochemical test of capacity and cycling performance, FeCl_3 , FeCl_2 , and MnCl_2 were screened out from the electrode candidates, and CoCl_2 and NiCl_2 were selected.

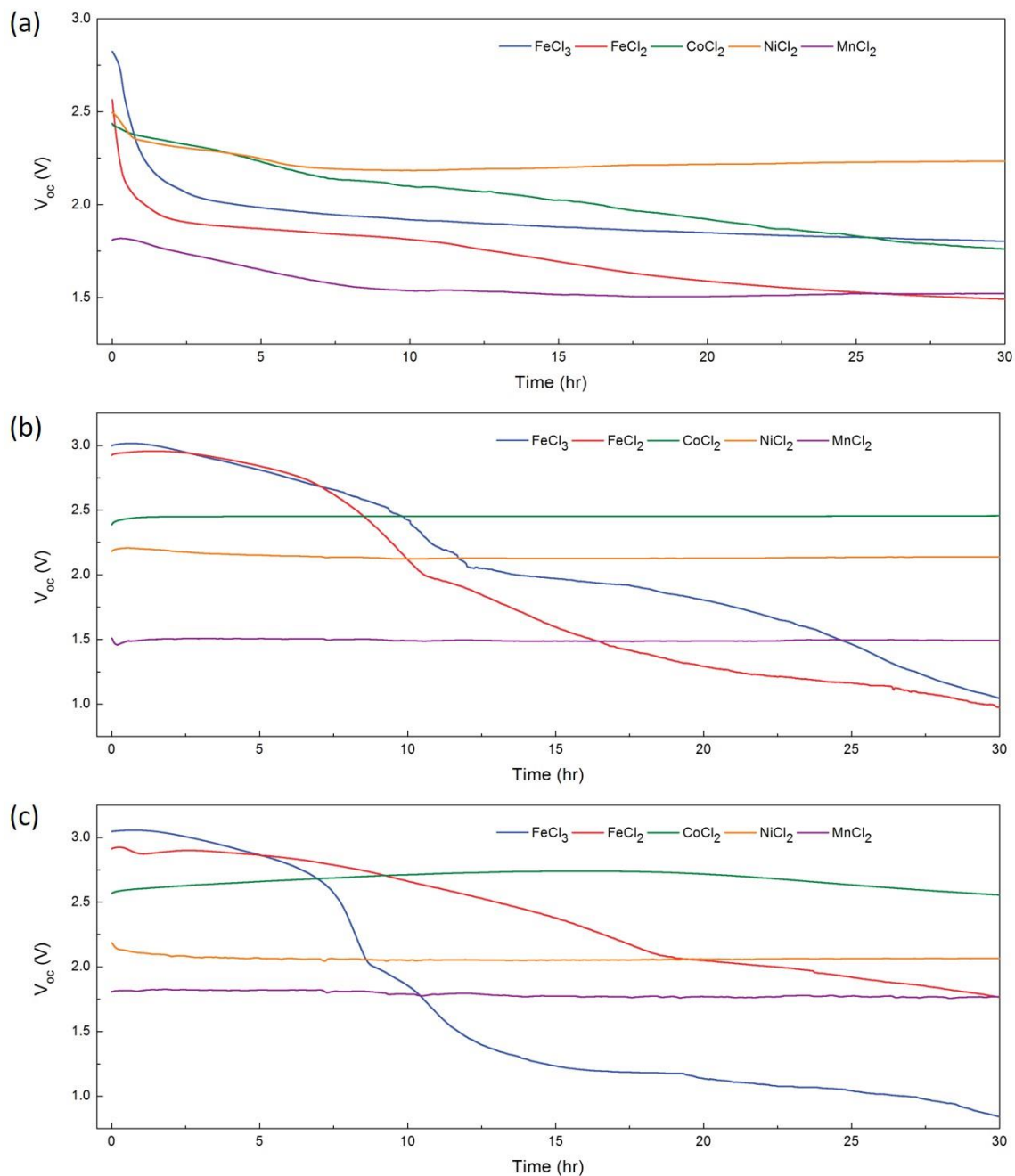


Figure 2.2 Open Circuit Voltage (OCV) of metal chloride materials in (a) reference electrolyte, (b) 0.1M LiCl/6M LiTFSI TEGDME, and (c) 0.1M LiCl/0.1M LiNO₃/6M LiTFSI TEGDME

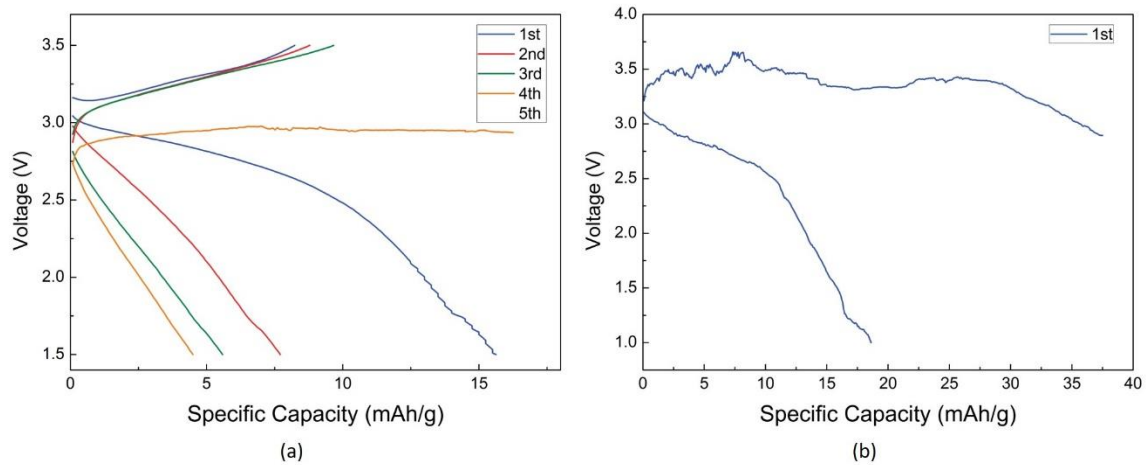


Figure 2.3 Voltage profile of FeCl_3 in (a) 0.1M LiCl/6M LiTFSI TEGDME, and (b) 0.1M LiCl/0.1M LiNO₃/6M LiTFSI TEGDME

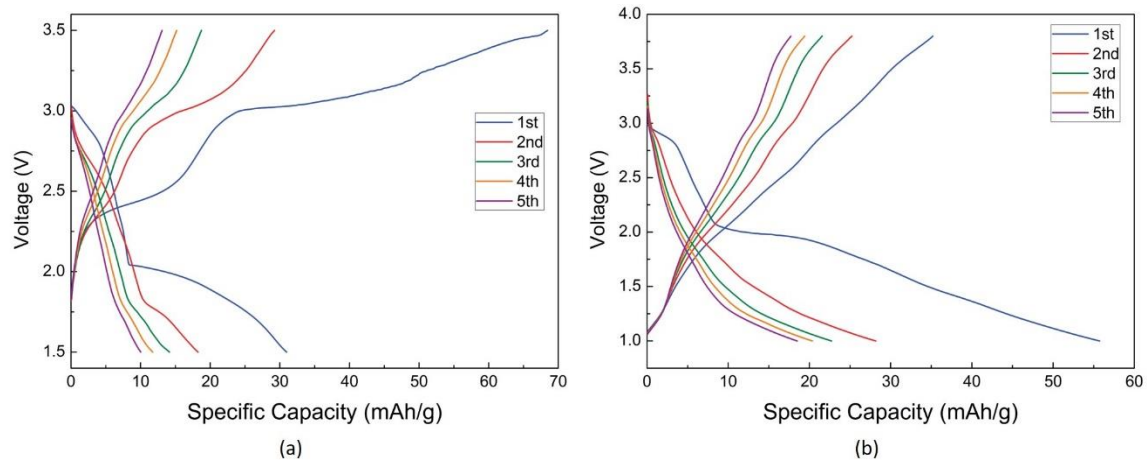


Figure 2.4 Voltage profile of FeCl₂ in (a) 0.1M LiCl/6M LiTFSI TEGDME, and (b) 0.1M LiCl/0.1M LiNO₃/6M LiTFSI TEGDME

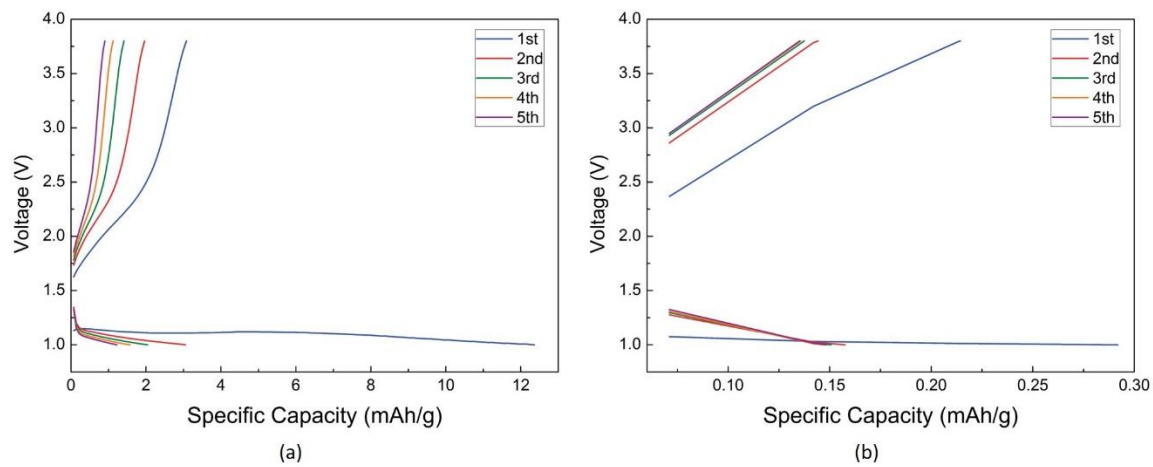


Figure 2.5 Voltage profile of MnCl_2 in (a) 0.1M LiCl/6M LiTFSI TEGDME, and (b) 0.1M LiCl/0.1M LiNO₃/6M LiTFSI TEGDME

2.2.3. Electrochemical Analysis

After screening out FeCl_3 , FeCl_2 , and MnCl_2 , CoCl_2 and NiCl_2 were electrochemically tested in reference electrolyte, superconcentrated electrolyte, and superconcentrated electrolyte containing LiNO_3 additive. Each cell was tested with 1/100 C from 1.0 V to 3.8 V cutoff voltage range. CoCl_2 in reference electrolyte showed 15 mAh g^{-1} at its first discharge, but it did not charge back, which means the cell lost CoCl_2 cathode material by dissolution (Fig. 2.6 (a)). When electrolyte was treated with high concentrations of LiTFSI salt, the capacity increased to 35 mAh g^{-1} at its first discharge, but it dropped below 15mAh g^{-1} from the second cycle (Fig. 2.6 (b)). Unlike in the reference electrolyte, the cell went through three cycles, but it failed cycling after the third cycle. This indicates that the superconcentrated electrolyte suppressed the dissolution of CoCl_2 , but it did not stop material loss completely. When current passes through the electrodes, unstable conversion reaction occurs, resulting in cathode material loss. Also, the polarization increased significantly after the first cycle. This indicates that after the first cycle, CoCl_2 material loss occurred severely, and the electrolyte became resistive, causing poor internal cell performance. The same electrochemical test was performed using concentrated electrolyte with LiNO_3 additive as seen in Fig. 2.6 (c). The first discharge capacity was 160 mAh g^{-1} which was ~40 % of theoretical capacity. After the first cycle, the capacity dropped continuously, but maintained a capacity of 60 mAh g^{-1} at the 5th cycle. Also, the cell had a lower polarization than (a) and (b), leading us to assume, a SEI layer formed because of the additive LiNO_3 resulting in improved cell performance. When dissolved CoCl_2 species migrate to anode lithium surface, they will negatively affect the SEI layer and form an unfavorable surface layer that causes ionic blockage^[15]. However, a

favorable SEI layer with N-O bonds prevents those negative phenomena, resulting in cell improvement. Capacity and coulombic efficiency by cycles are plotted in Fig. 2.7 for both superconcentrated electrolyte without (a), and with LiNO_3 (b). Coulombic efficiency was maintained over 100 % after the third cycle in (b), and the first three cycles had over 90 % efficiency. The efficiency was over 100 % because CoCl_2 already formed Co metal by spontaneous reduction before its first discharge (see below). Since more Co metal exists in the electrode, charging time was greater than discharging time. For the first few cycles, the experimental capacity did not meet the theoretical maximum so that the efficiency was not over 100 %, but once it stabilized to the utilized amount of its actual active material, the amount of Co might be greater than CoCl_2 material. We further structurally characterized the electrode to confirm the idea (shown in the next section). The capacity dropped crucially during the first five cycles due to high polarization and the material loss. However, since the lithium surface was protected by SEI layer formed by LiNO_3 , the capacity drop stabilized between 60 to 30 mAh g^{-1} . This indicates that LiNO_3 does not help suppress the cathode material dissolution, but does form a passivation layer on the lithium anode.

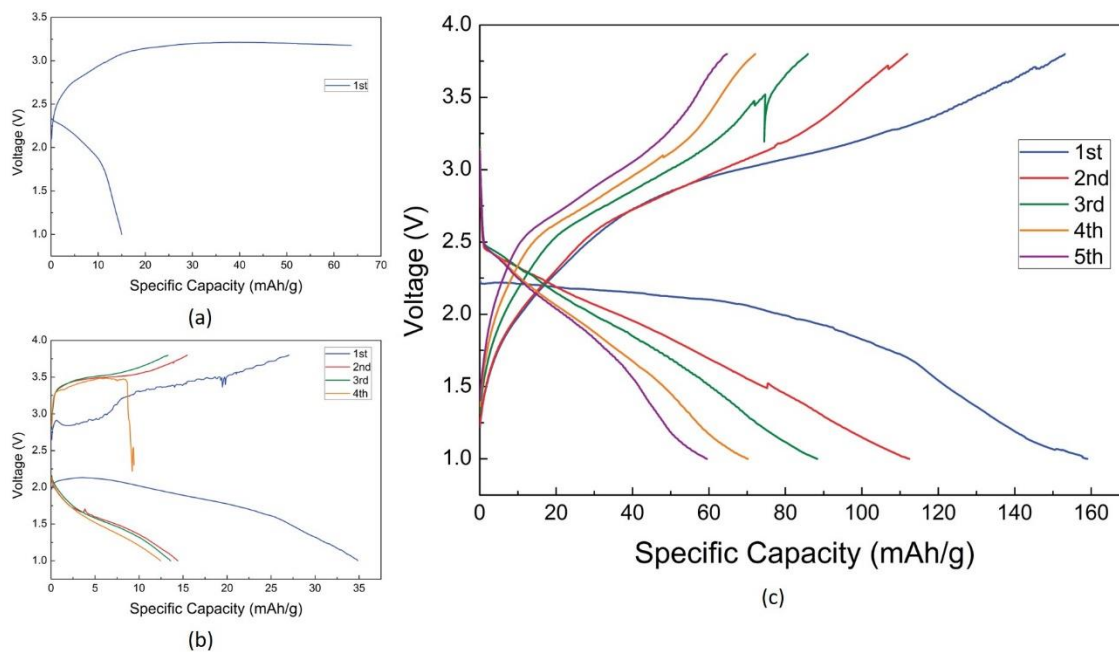


Figure 2.6 Voltage profile of CoCl_2 in (a) reference electrolyte, (b) 0.1M LiCl/6M LiTFSI TEGDME, and (c) 0.1M LiCl/0.1M LiNO₃/6M LiTFSI TEGDME

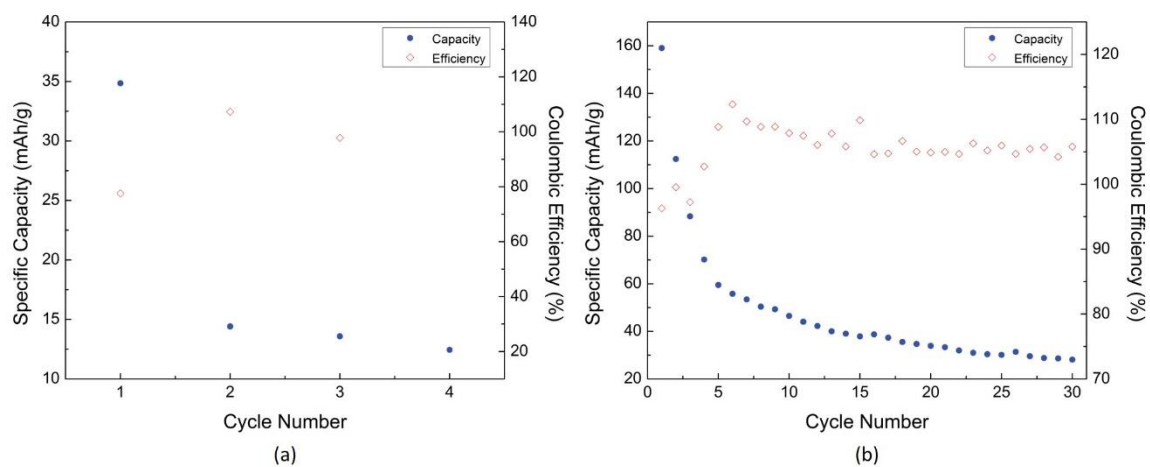


Figure 2.7 Cycling performance of CoCl₂ in (a) 0.1M LiCl/6M LiTFSI TEGDME, and (b) 0.1M LiCl/0.1M LiNO₃/6M LiTFSI TEGDME

Cell experiments have been done with NiCl_2 under the identical conditions as CoCl_2 test. When NiCl_2 was tested in the reference electrolyte (Fig. 2.8 (a)), the capacity hit 320 mAh g^{-1} which was 77 % of theoretical value at its first discharge. It also had a stable plateau maintained at over 2.0 V. This is because the electrolyte has lower viscosity than concentrated ones, and its ionic conductivity is higher than the others. However, the cell failed to charge back. The cell discharged stably at its first discharge, but showed irreversible material loss after being reduced during the conversion reaction. When NiCl_2 was tested in the superconcentrated electrolyte without LiNO_3 additive, the cell showed better cyclability. The first discharge capacity was $\sim 170 \text{ mAh g}^{-1}$ which was ~ 40 % of theoretical value. The first discharge capacity was higher than the first charge capacity because it favored the reduction of NiCl_2 , but it did not maintain 100 % reversibility. However, after few cycles, the reaction stabilized and showed high coulombic efficiency close to 100 %. Polarization is still an unsolved problem in conversion reactions. Also the capacity drop was still significant at the first few cycles by the degradation of NiCl_2 , but the capacity range became stabilized between 80 to 40 mAh g^{-1} . When LiNO_3 additive was added (Fig. 2.8 (c)), the cell performance drastically improved. The first discharge capacity was 330 mAh g^{-1} which was 80% of theoretical value, and the conversion reaction occurred stably throughout the cycles. After the first cycle, capacity dropped to below 200 mAh g^{-1} , but the cell became stable. Due to the high cell viscosity and the intrinsic conversion mechanism, polarization was still high. During the first discharge, Ni metal formed more than the NiCl_2 formation in the later oxidation reaction, and it was expected that Ni metal still exists after charging back. Further characterization of the metal exists in the later sections. Similar as in other electrolytes, discharge capacity dropped significantly

at the beginning of the cycling (Fig. 2.9 (b)). From the second to 15th cycle, capacity drop was not critical, but from 16th cycle, capacity stepped down below 100 mAh g⁻¹. However, coulombic efficiency maintained over 95% throughout the whole discharge/charge performance. Therefore, LiNO₃ protects the lithium surface from the dissolved NiCl₂ species as well, and allows the stable conversion reactions during discharge/charge. **NiCl₂ as a cathode material and 0.1M LiCl/0.1M LiNO₃/6M LiTFSI TEGDME as a combinational electrolyte showed the best performance with high capacity and stable cyclability.**

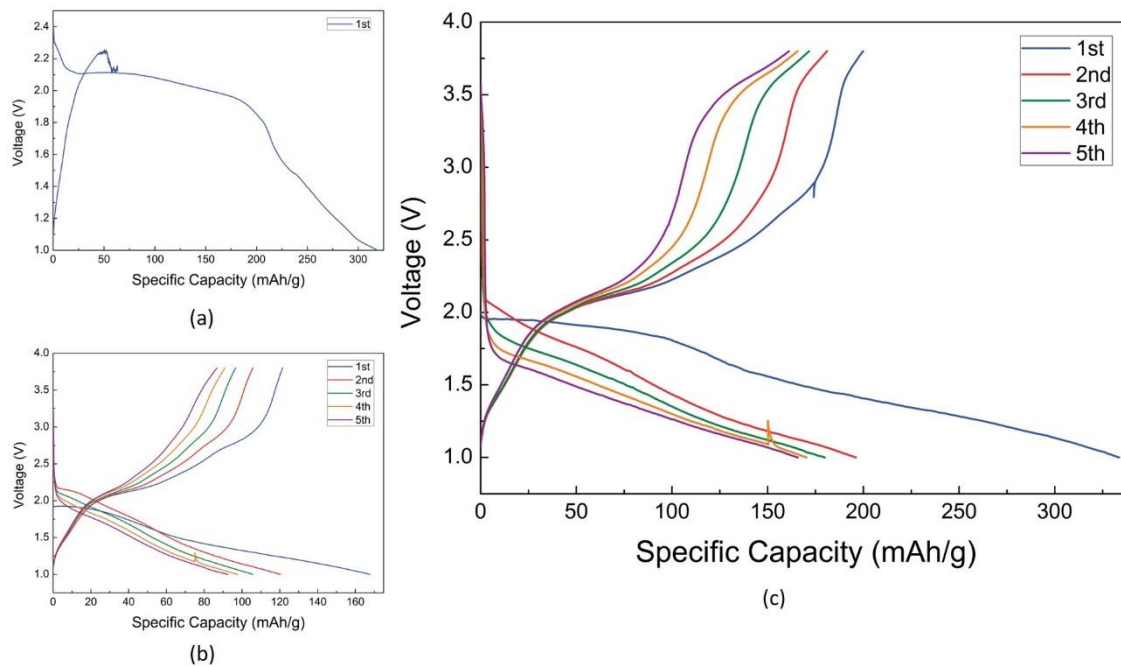


Figure 2.8 Voltage profile of NiCl_2 in (a) reference electrolyte, (b) 0.1M LiCl/6M LiTFSI TEGDME, and (c) 0.1M LiCl/0.1M LiNO₃/6M LiTFSI TEGDME

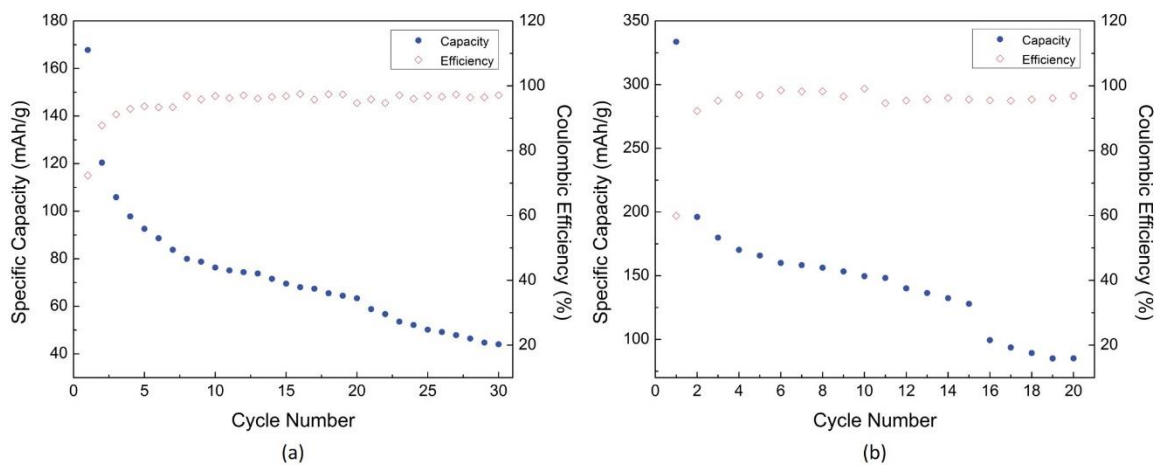


Figure 2.9 Cycling performance of NiCl₂ in (a) 0.1M LiCl/6M LiTFSI TEGDME, and (b) 0.1M LiCl/0.1M LiNO₃/6M LiTFSI TEGDME

Galvanostatic Intermittent Titration Technique (GITT) was performed to detect the average potential and discharge/charge potentials (Fig. 2.10) by 1/100 C within cutoff voltage at 1.0 V and 3.8 V. For CoCl_2 (Fig. 2.10 (a)), the voltage at rest was ~ 2.4 V, while theoretical voltage was 2.59 V. During discharge the voltage dropped fast unlike with continuous current. This result interprets that CoCl_2 degradation is time dependent since GITT measures the voltage stability by resting, and during that time, degradation of CoCl_2 occurred. Discharge to 1.0 V took over 100 h, and during that time side reaction of CoCl_2 conversion material most likely occurred, the reaction became irreversible causing high polarization. This promoted the fast degradation of CoCl_2 and did not charge back to 3.8 V. For NiCl_2 (Fig. 2.10 (b)), the voltage at rest was ~ 2.2 V, while theoretical average voltage is 2.64 V. NiCl_2 had a relatively smaller polarization than CoCl_2 , showing discharge voltage at ~ 2.0 V. Charge voltage was at ~ 2.7 V and the voltage at rest during charging varied from 2.1 V to 2.6 V, which implies that an irreversible reaction of NiCl_2 also occurred. The voltage difference between relaxation and discharge was 0.2 V with stable plateau. This low polarization shows great promise of NiCl_2 for a cathode material. Hysteresis is ~ 0.5 V during the cycle indicating that NiCl_2 is more advantageous than FeF_3 , which has a hysteresis over 1 V^[14]. NiCl_2 did not completely lose reversibility unlike CoCl_2 , indicating also that NiCl_2 is more stable conversion cathode material in superconcentrated electrolyte than CoCl_2 .

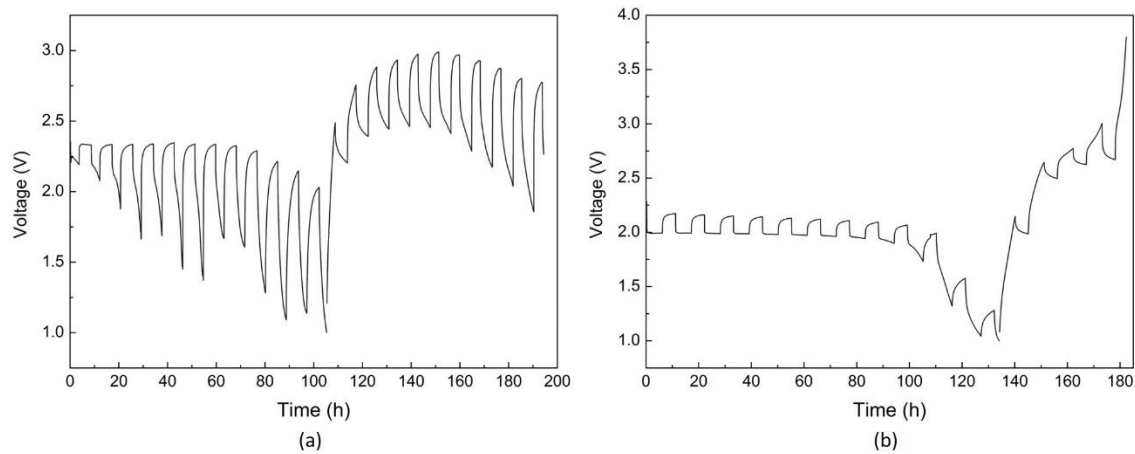


Figure 2.10 Galvanostatic Intermittent Titration Technique (GITT) of (a) CoCl₂, and (b) NiCl₂ in 0.1M LiCl/0.1M LiNO₃/6M LiTFSI TEGDME

2.2.4. Characterizations

To characterize the conversion reaction of CoCl_2 and NiCl_2 , *ex situ* X-Ray Diffraction (XRD) was used to detect the crystals formed in the samples (Fig. 2.11). However, since metal chloride materials are well dissolved in N-methyl-2-pyrrolidone (NMP)^[36], materials lost their crystallinity or became amorphous, therefore XRD did not show very much intensity and could not detect sharp peaks. From the XRD result of CoCl_2 in Fig. 2.11 (a), undesired materials were produced when CoCl_2 was used as an electrode material. It was reported that Cobalt (II) reacts with NMP at 75 °C under 3.4 atm of oxygen, and produce N-methylsuccinimide (NMSI). NMP decomposed to NMSI even more rapidly at higher temperatures^[37]. During the electrode slurry process, CoCl_2 was added in NMP solvent and dried at 120 °C and 5 atm with tiny amount of oxygen residue in the glove box. During the slurry process under a great condition of NMP oxidation, it was partially reducing CoCl_2 to Co, and Cobalt (II) oxidized NMP to produce NMSI. Therefore, reduced Co metal and other side products coexist in the as-prepared electrode. Since the electrode became amorphous, Co metal and CoCl_2 were not detectable after discharged or after charge. Moreover, the LiCl product of the conversion reaction: $\text{CoCl}_2 + 2 \text{Li}^+ \rightarrow \text{Co} + 2 \text{LiCl}$, is well-known amorphous nano-particles smaller than the X-ray coherence length^[36], and thus, XRD could not detect LiCl particles as well. XRD patterns show that NiCl_2 is more stable in NMP than CoCl_2 . NiCl_2 in as-prepared electrode were showing similar peaks as NiCl_2 powder, proving that there was no side reactions between NiCl_2 and NMP, and it was expected that there will not be metals formed in the as-prepared electrode. However, since conversion materials often lose their crystallinity during the reactions, NiCl_2 also did not show clear peaks after discharge, and it was not able to confirm that Ni metal formed.

When the cell charged back, it was expected to detect NiCl_2 . At the recharged electrode, few peaks were detectable at 32° and 37.8° , located at the same diffraction angle as NiCl_2 broad peaks. When it oxidized back to NiCl_2 , it is possible that the reproduced particles have preferred orientation, or it formed large size (i.e., thousands of unit cells) of crystals that cancel the other diffractions by incoherent scattering, but have a strong coherent scattering with in a big structure^[38].

Owing to the difficulty of detecting metal particles by *ex situ* XRD, Vibrating Sample Magnetometer (VSM) was performed to confirm the metal formation during conversion reactions (Fig. 2.12 and 2.13). Since VSM measures the magnetic moment and coercivity of the ferromagnetic materials such as Co and Ni, and it does not detect antiferromagnetic materials such as CoCl_2 and NiCl_2 , making it a great technique to detect the Co and Ni metal formations^[39]. In this test, it was rather intuitive approach to confirm the metal formation in as-prepared electrodes, discharged electrodes, and recharged electrodes of CoCl_2 and NiCl_2 . Fig. 2.12 shows VSM test of CoCl_2 electrode. In the previous discussions, it was expected Co metal to exist in the as-prepared electrode since CoCl_2 reacts with NMP and it is reduced to produce Co metal. Fig. 2.12 (a) proved that the as-prepared electrode has a ferromagnetic metal in the specimen, having sharp moment change near zero magnetic field. When the cell discharged in Fig. 2.12 (b), it also detected Co metals, but the coercivity increased, which means Co metal particles have a bigger size after discharge. When the cell charged back, Co metals reversibly went back to form CoCl_2 , and the plot had a moderate “S” shape rather than sharp stiffness. This implies that the sample contained both ferromagnetic and antiferromagnetic materials. Since Co metal did not have a 100 % reversibility, there were still Co metal exists in the electrode.

NiCl₂ electrodes were tested with VSM as well. Since NiCl₂ was stable with NMP, it was expected that as-prepared electrode has no Ni metals, but only NiCl₂ antiferromagnetic materials. Likely, the Fig. 2.13 (a) shows only antiferromagnetic response, which proves that there were no side reactions between NiCl₂ and NMP and a metal formation. After discharged in the Fig. 2.13 (b), Ni metal formed by the conversion reaction was detected. However, the plot did not show the sharp steepness near zero magnetic field, which means the reaction yield was not 100 %, and there were still antiferromagnetic material left. Similarly, when it charged back, not all the Ni metal turned back to NiCl₂, and it still had a high moment. However, since the reaction successfully occurred, the plot of recharged electrode has more linear “S” shape than that of discharged electrode that contains more Ni metal.

Unlike NiCl₂, CoCl₂ had a side reaction with NMP, and it was unclear if the actual active material had a conversion reaction. To support the conversion reaction of CoCl₂, Fourier-transform infrared spectroscopy (FT-IR) was performed to detect the LiCl formation and the change of CoCl₂ level (Fig. 2.14). The major peak of CoCl₂ was at 1600 cm⁻¹, and that of LiCl was at 1630 cm⁻¹ and 1656 cm⁻¹. As discussed before, as-prepared CoCl₂ electrode was expected to have both CoCl₂ and LiCl peaks since CoCl₂ was partially reduced to form Co and LiCl, and the electrode had peaks at ~1630 cm⁻¹ and ~1600 cm⁻¹. When the cell discharged, the peak at 1630 cm⁻¹ drastically increased, on the other hand, the peak at 1600 cm⁻¹ disappeared, which proves that LiCl has produced dominantly coming up with Co metal. Moreover, after charged back, the peak at 1630 cm⁻¹ disappeared, and a majority of the peaks was located at 1600 cm⁻¹. This is telling that during recharging,

the reversible conversion reaction occurred, and produced CoCl_2 , but it still had some minor peaks of LiCl .

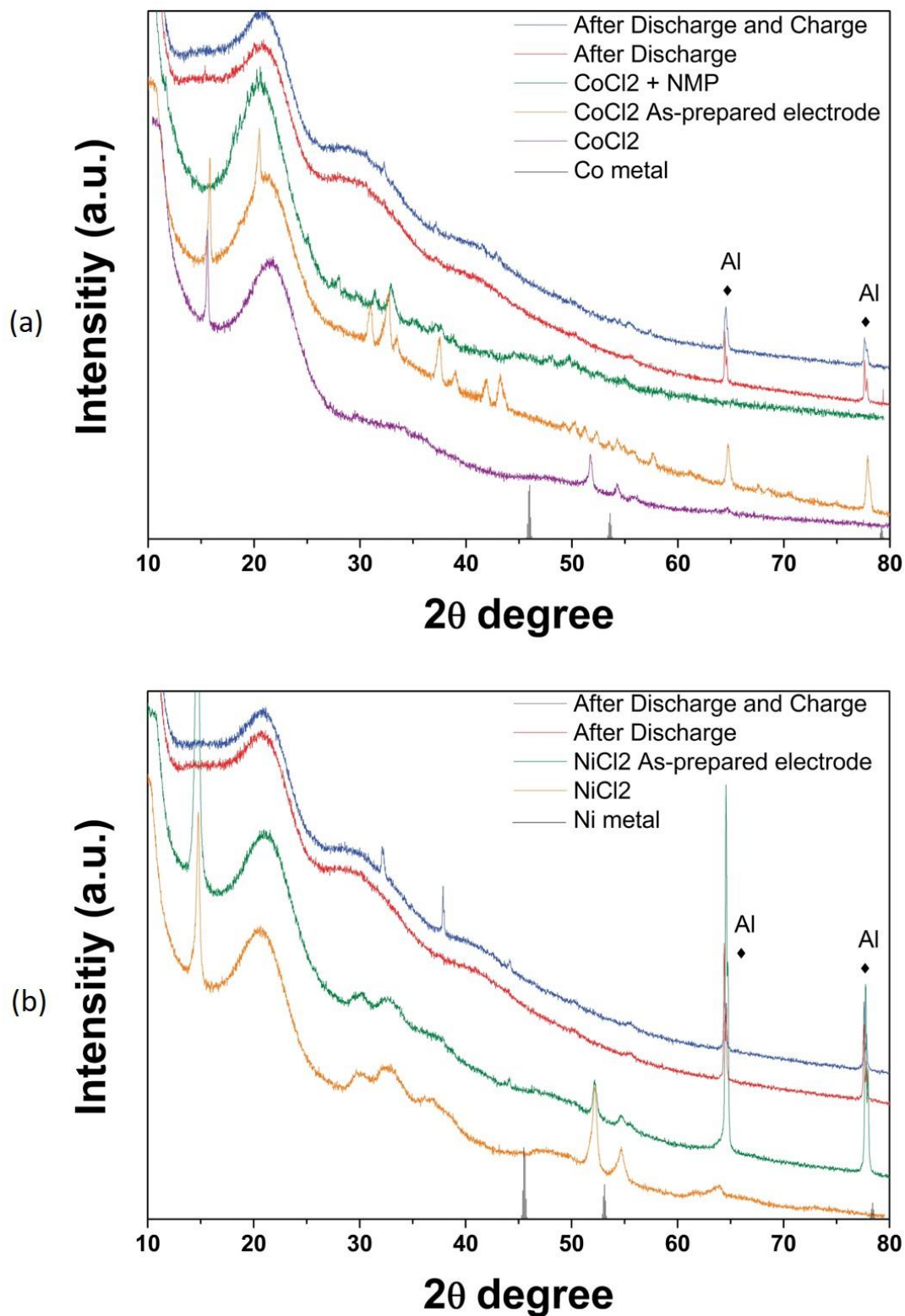


Figure 2.11 X-Ray Diffraction (XRD) characterizations of (a) CoCl₂, and (b) NiCl₂

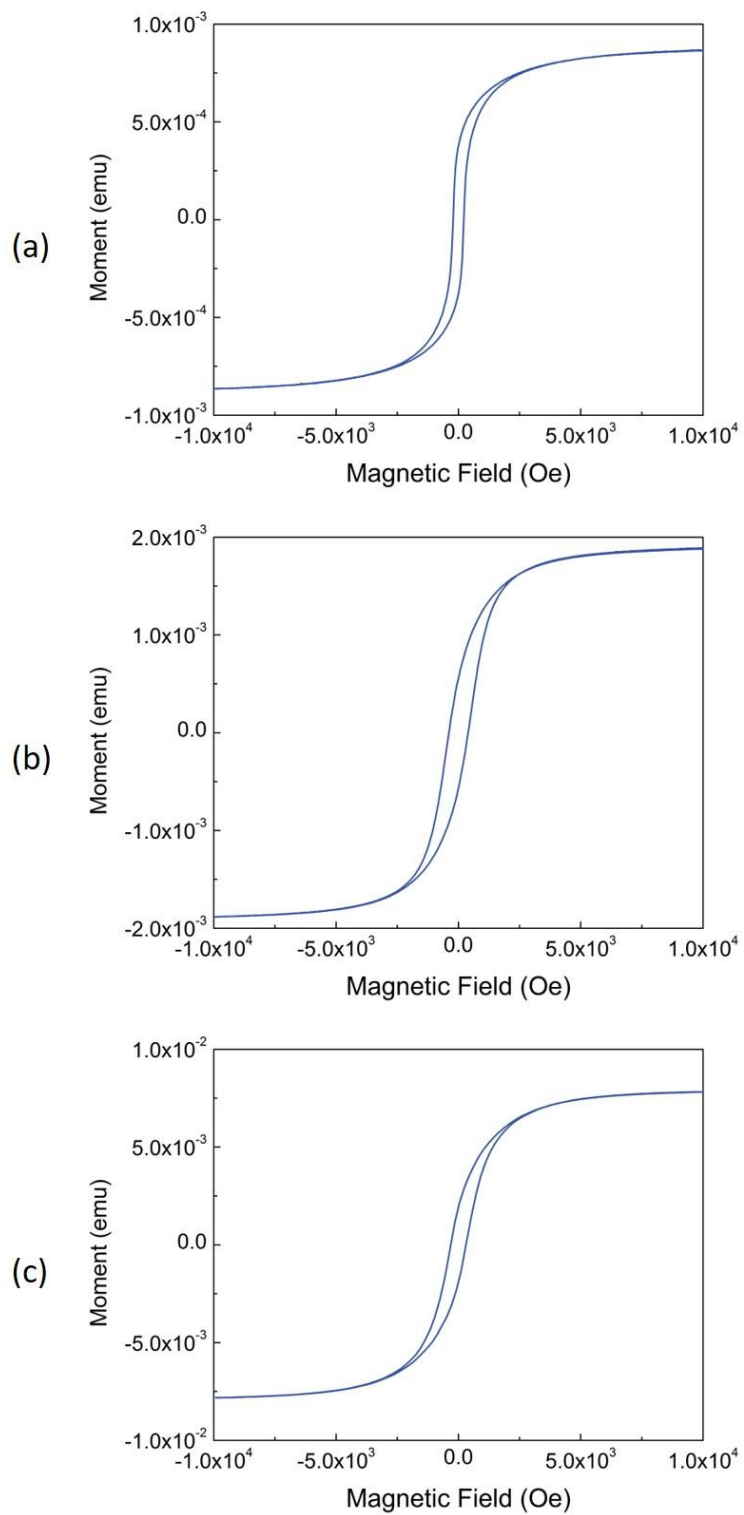


Figure 2.12 Vibrating Sample Magnetometer (VSM) characterizations of CoCl_2 of (a) as prepared electrode, (b) after discharged, (c) after recharged

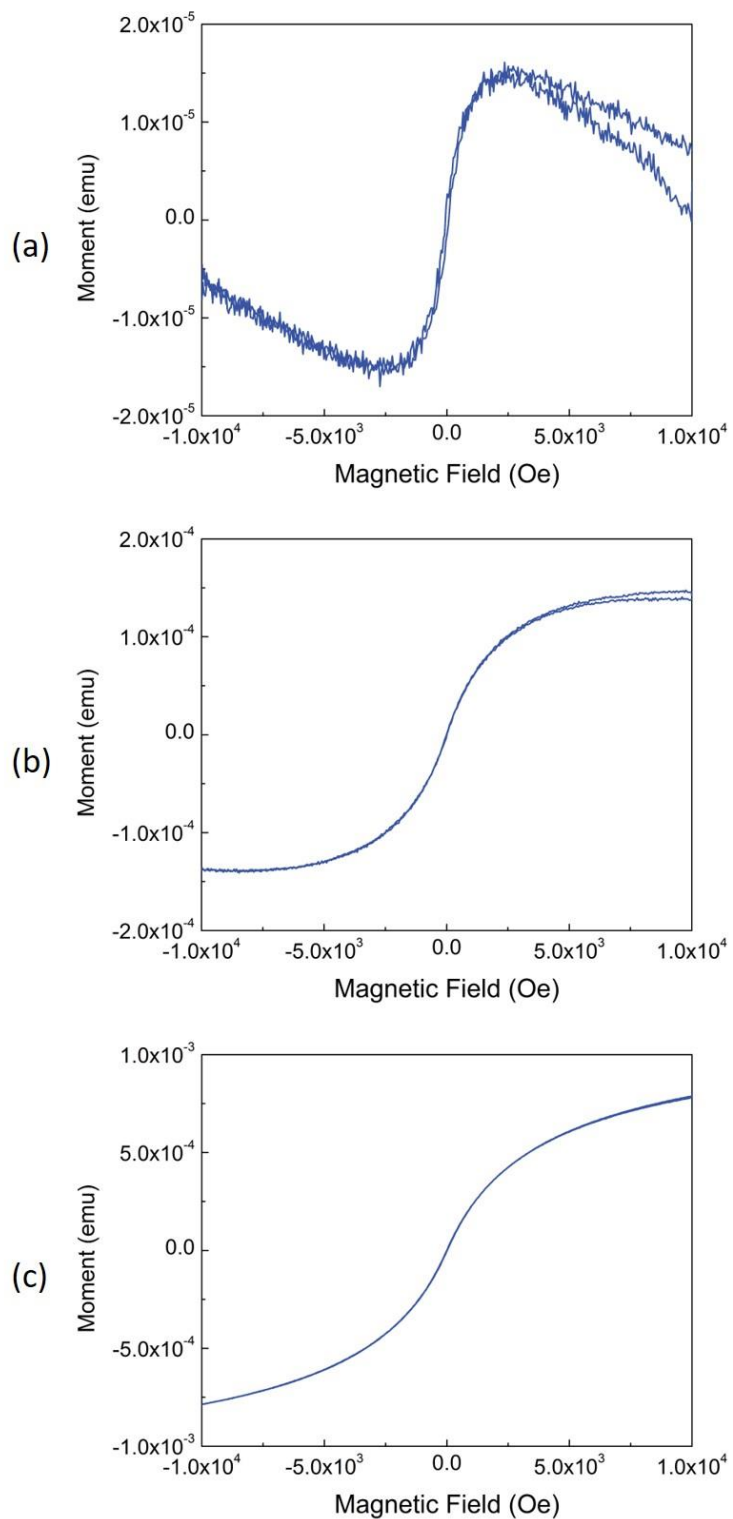


Figure 2.13 Vibrating Sample Magnetometer (VSM) characterizations of NiCl_2 of (a) as prepared electrode, (b) after discharged, (c) after recharged

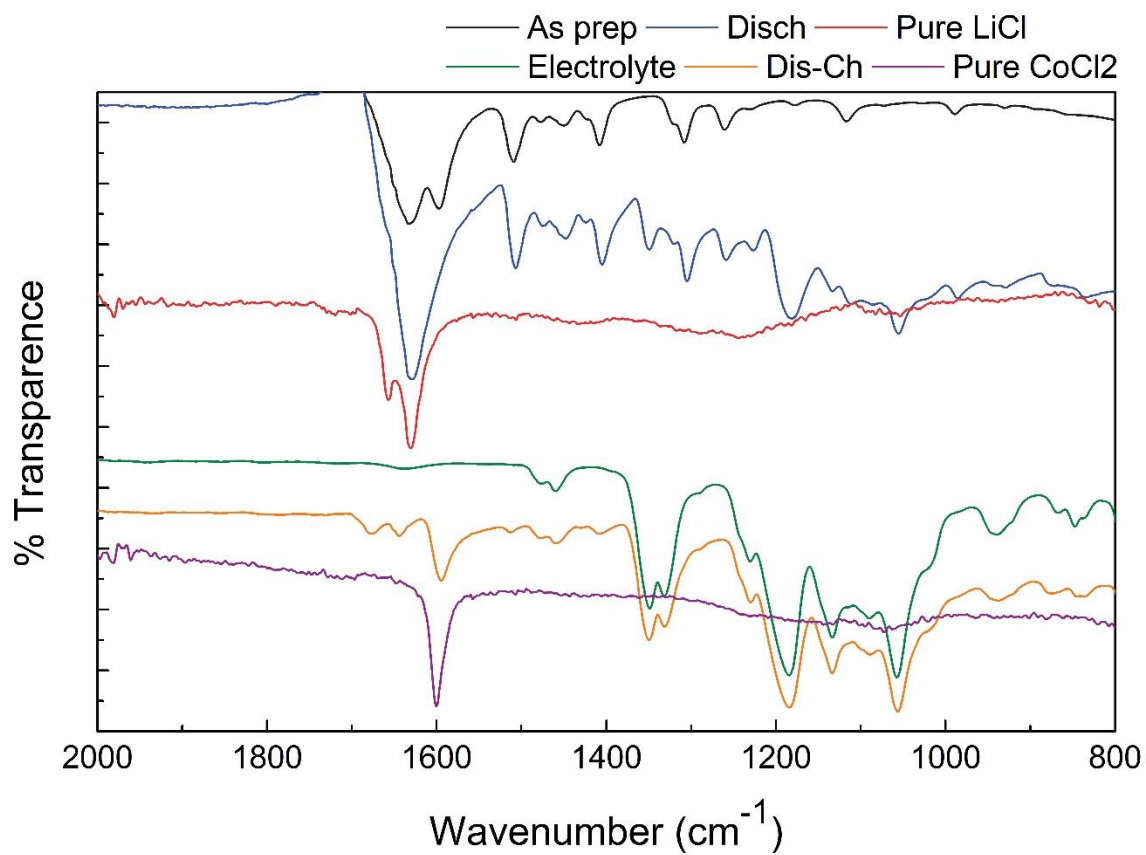


Figure 2.14 Fourier-Transform Infrared Spectroscopy (FT-IR) of CoCl_2

2.3. Methods

Preparation of Electrodes and Electrolytes

99.99 % anhydrous FeCl_3 , 99.99 % anhydrous FeCl_2 , 98.0 % anhydrous CoCl_2 , 98% anhydrous NiCl_2 , and 99.99% anhydrous MnCl_2 were purchased from Sigma-Aldrich, and LP 30 (EC:DMC = 1:1 w/ LiPF_6) and Dimethoxyethane (DME) were purchased from BASF. 99.0 % Tetraethylene glycol dimethyl ether (TEGDME) was purchased from Sigma-Aldrich. Lithium nitrate (LiNO_3) was purchased from Sigma-Aldrich, and lithium chloride (LiCl) was purchased from Calbiochem. Each electrode was prepared by 80 % of active material, 10 % of Super P carbon black, and 10 % of PVdF-HFP binder in NMP solvent. The sluggish electrodes were dried at 120 °C in the glove box. Reference electrolyte was made with 1M of LiTFSI in TEGDME, and two other conditioned electrolytes were treated by 0.1M $\text{LiCl}/6\text{M}$ LiTFSI in TEGDME and 0.1M $\text{LiCl}/0.1\text{M}$ $\text{LiNO}_3/6\text{M}$ LiTFSI in TEGDME. For the experimental electrolyte group, 0.1M was maximum dissolution concentration for LiCl , and 6M was for LiTFSI. For the superconcentrated electrolytes, heat was applied when dissolved LiTFSI at 50 °C.

Electrochemical Measurements

Electrochemical measurements were conducted by Arbin. Open Circuit Voltage (OCV) was tested for 30 h for each cell. For the voltage profile and cycling performance, current applied by 1/100 C, and the cut-off voltage was lowest at 1.0 V and highest at 3.8 V. GITT was tested for CoCl_2 and NiCl_2 in 0.1M $\text{LiCl}/0.1\text{M}$ $\text{LiNO}_3/6\text{M}$ LiTFSI TEGDME electrolyte at 1/100 C. Cut-off voltage was also lowest at 1.0 V and highest at 3.8 V. The

running time for CoCl_2 and NiCl_2 was 3.5 h and 6 h, respectively. The rest time for both CoCl_2 and NiCl_2 was 5 h each.

2.4. Conclusion

Metal chloride conversion cathode materials are promising cathode materials in Li-ion batteries due to their high capacity and energy density properties. However, the conversion cathode materials face a critical challenge to overcome: active material loss. Since metal chlorides are strongly dissolved in the electrolyte, suppressing dissolution was mainly focused in this paper.

Through a two-step screening of transition metal chloride materials and electrolyte solvents, CoCl_2 and NiCl_2 were selected as promising cathode materials. Highly concentrated electrolytes that consist of 0.1M LiCl/6M LiTFSI and 0.1M LiCl/0.1M LiNO_3 /6M LiTFSI in TEGDME solvent proved to effectively suppress the dissolution of cathode materials. Electrochemical test and cell characterizations were carried out to measure the performance of metal chloride materials as new Li-ion battery cathodes. LiNO_3 additive increased the cell capacity up to 40 % and 80 % in both CoCl_2 and NiCl_2 respectively, and a passivation layer on lithium surface allowed for stable cell cycling. The metal chloride materials were characterized by XRD, VSM, and FT-IR. However, since metal chloride materials are easily dissolved in NMP solvent, they become amorphous, discharged and recharged electrodes could not be clearly characterized through XRD. As-prepared electrode of CoCl_2 showed some unidentified peaks, but we conclude that CoCl_2 reacted with NMP under desired conditions and produced Co metal. On the other hand, NiCl_2 was stable in NMP, and we conclude that NiCl_2 did not have a side reaction. The

conversion reactions were confirmed by VSM and FT-IR. VSM detected the metal in the as-prepared electrode of CoCl_2 , and showed clear change in the metal state and coercivity. For NiCl_2 , no Ni metal was detected in as-prepared, but Ni metal was detected after discharged and recharged. FT-IR characterization further supports the idea that CoCl_2 formed Co metal in as-prepared samples by showing co-exist of CoCl_2 and LiCl product. During discharge, LiCl level increased but CoCl_2 disappeared. When charged back, CoCl_2 increased and LiCl disappeared.

Through proper treatments of electrolyte, we effectively suppressed the dissolution of CoCl_2 and NiCl_2 . However, some other problems such as high polarizations, low ionic conductivity, drastic capacity drops, and incomplete dissolution suppression remain to be resolved by the further research. Although the mechanism has not been proved yet, NiCl_2 shows promise with its relatively small hysteresis (~ 0.5 V) and polarization (~ 0.2 V during discharge) unlike high hysteresis metal fluoride materials (over 1 V), making it worthwhile to further investigate. Ultimately, high capacity and energy density metal chloride cathode present a great new concept to replace current low capacity cathode materials if the major problems can be resolved.

References

- [1] J. K. Park, *Principles and Applications of Lithium Secondary Batteries*, Wiley, **2012**.
- [2] Emaze, **2017**, Available from: <https://www.emaze.com/@ACCLCQFC/Sharvanti>.
- [3] V. Etacheri, R. Marom, R. Elazari, G. Salitra, D. Aurbach, *Energy Environ. Sci.* **2011**, 4, 3243.
- [4] K. Mizushima, P. Jones, P. Wiseman, J. B. Goodenough, *Materials Research Bulletin* **1980**, 15, 783.
- [5] M. Winter, J. O. Besenhard, M. E. Spahr, P. Novák, *Adv. Mater.* **1998**, 10, 725.
- [6] Y. M. Lee, J. Y. Lee, H.-T. Shim, J. K. Lee, J.-K. Park, *J. Electrochem. Soc.* **2007**, 154, A515.
- [7] C. K. Chan, H. Peng, G. Liu, K. McIlwrath, X. F. Zhang, R. A. Huggins, Y. Cui, *Nature nanotechnology* **2008**, 3, 31.
- [8] A. S. Aricò, P. Bruce, B. Scrosati, J.-M. Tarascon, W. Van Schalkwijk, *Nat. Mater.* **2005**, 4, 366.
- [9] B. Philippe, R. m. Dedryvère, M. Gorgoi, H. k. Rensmo, D. Gonbeau, K. Edström, *Chem. Mater.* **2013**, 25, 394.
- [10] S. F. Lux, J. Chevalier, I. T. Lucas, R. Kostecki, *ECS Electrochemistry Letters* **2013**, 2, A121.
- [11] J.-M. Tarascon, M. Armand, *Nature* **2001**, 414, 359.
- [12] M. R. Palacin, *Chem. Soc. Rev.* **2009**, 38, 2565.
- [13] R. Malini, U. Uma, T. Sheela, M. Ganesan, N. Renganathan, *Ionics* **2009**, 15, 301.
- [14] P. Liu, J. J. Vajo, J. S. Wang, W. Li, J. Liu, *J. Phys. Chem. C* **2012**, 116, 6467.
- [15] F. Wu, G. Yushin, *Energy Environ. Sci.* **2017**, 10, 435.
- [16] N. Nitta, F. Wu, J. T. Lee, G. Yushin, *Materials today* **2015**, 18, 252.
- [17] R. Miao, J. Yang, Z. Xu, J. Wang, Y. Nuli, L. Sun, *Sci. Rep.* **2016**, 6, 21771.

- [18] E. S. Shin, K. Kim, S. H. Oh, W. I. Cho, *Chem. Commun.* **2013**, 49, 2004.
- [19] L. Suo, Y.-S. Hu, H. Li, M. Armand, L. Chen, *Nat. Commun.* **2013**, 4, 1481.
- [20] J. T. Lee, Y. Zhao, S. Thieme, H. Kim, M. Oschatz, L. Borchardt, A. Magasinski, W. I. Cho, S. Kaskel, G. Yushin, *Adv. Mater.* **2013**, 25, 4573.
- [21] K. Ueno, J.-W. Park, A. Yamazaki, T. Mandai, N. Tachikawa, K. Dokko, M. Watanabe, *J. Phys. Chem. C* **2013**, 117, 20509.
- [22] J. Wang, Y. Yamada, K. Sodeyama, C. H. Chiang, Y. Tateyama, A. Yamada, **2016**, 7, 12032.
- [23] S. E. Sloop, J. K. Pugh, S. Wang, J. Kerr, K. Kinoshita, *Electrochem. Solid State Lett.* **2001**, 4, A42.
- [24] E. Cho, J. Mun, O. B. Chae, O. M. Kwon, H.-T. Kim, J. H. Ryu, Y. G. Kim, S. M. Oh, *Electrochem. Commun.* **2012**, 22, 1.
- [25] R. Younesi, G. M. Veith, P. Johansson, K. Edström, T. Vegge, *Energy Environ. Sci.* **2015**, 8, 1905.
- [26] J. Li, C. Daniel, D. Wood, *J. Power Sources* **2011**, 196, 2452.
- [27] Y. Yamada, A. Yamada, *J. Electrochem. Soc.* **2015**, 162, A2406.
- [28] S. S. Zhang, J. A. Read, *J. Power Sources* **2012**, 200, 77.
- [29] Y.-S. Su, Y. Fu, T. Cochell, A. Manthiram, *Nat. Commun.* **2013**, 4, 2985.
- [30] H. S. Kim, T.-G. Jeong, N.-S. Choi, Y.-T. Kim, *Ionics* **2013**, 19, 1795.
- [31] Y. V. Mikhaylik, U.S. Patent, 7,352,680, 2008.
- [32] D. Aurbach, E. Pollak, R. Elazari, G. Salitra, C. S. Kelley, J. Affinito, *J. Electrochem. Soc.* **2009**, 156, A694.
- [33] X. Liang, Z. Wen, Y. Liu, M. Wu, J. Jin, H. Zhang, X. Wu, *J. Power Sources* **2011**, 196, 9839.
- [34] S. S. Zhang, *J. Electrochem. Soc.* **2012**, 159, A920.
- [35] X. Ji, K. T. Lee, L. F. Nazar, *Nat. Mater.* **2009**, 8, 500.
- [36] J.-l. Liu, W.-j. Cui, C.-x. Wang, Y.-y. Xia, *Electrochem. Commun.* **2011**, 13, 269.

- [37] R. S. Drago, R. Riley, *J. Am. Chem. Soc.* **1990**, 112, 215.
- [38] R. James, *EPS400-002* **2012**.
- [39] B. D. Cullity, C. D. Graham, *Introduction to magnetic materials*, John Wiley & Sons, **2011**.